FRIGID ZONE **MEDICINE**
Original Article • DOI: 10.1515/fzm-2025-0019

Deficiency of LncRNA-CIRBIL promotes J-wave syndrome by enhancing transmural heterogeneity of I_{to} current: LncCIRBIL regulates J-wave syndrome *via* UPF1

Xuexin Jin[1,2#], Wenbo Ma[1#], Jinyun Guo[1#], Yueying Qu[1], Haiyu Gao[1], Dechun Yin[2], Desheng Li[1], Ling Shi[2], Jialiang Li[1], Jiudong Ma[1], Lingmin Zhang[1], Hongli Shan[3], Yanjie Lu[1,4], Yue Li[2,5*], Dongmei Gong[1*], Zhenwei Pan[1,4*]

Abstract

Background: Transmural heterogeneity of the transient outward potassium current (I_{to}) is a major contributor to J-wave syndrome (JWS). However, the underlying molecular mechanisms remain elusive. The present study aimed to investigate the role of cardiac injury-related bclaf1-interacting lncRNA (lncCIRBIL) in JWS and to delineate the molecular mechanisms. **Methods:** Whole-cell patch-clamp techniques were used to record ionic currents and action potentials (APs). Protein and mRNA expression related to Ito current were assessed. RNA immunoprecipitation, RNA Pulldown, mRNA stability, and decapping assays were performed to dissect the underlying mechanisms. **Results:** Plasma lncCIRBIL levels were significantly reduced in JWS patients and cold-induced JWS mice. Knockout of lncCIRBIL increased the incidence of J-wave and the susceptibility to ventricular arrhythmia in mice. In lncCIRBIL-deficient mice, the transmural gradient of Kv4.2 expression and Ito current density was markedly enhanced in the right ventricle, but not the left ventricle. In contrast, cardiomyocyte-specific transgenic overexpression of lncCIRBIL produced the opposite effects. In human induced pluripotent stem cell-derived cardiomyocytes (hiPSC-CMs), the conserved human homologous fragment of lncCIRBIL (hcf-CIRBIL) suppressed Ito, attenuated the AP notch, and prolonged APD20. Mechanistically, lncCIRBIL directly binds to up-frameshift protein1 (UPF1), promoting *KCND2* mRNA decay by enhancing its decapping. **Conclusions:** LncCIRBIL modulates the transmural heterogeneity of *KCND2* expression by regulating UPF1-mediated mRNA decay. Inhibition of lncCIRBIL exacerbates JWS by enhancing right ventricular Ito heterogeneity, whereas its overexpression exerts protective effects. These findings identify lncCIRBIL as a potential therapeutic target for J-wave syndrome.

Keywords

long noncoding RNA; J-wave syndrome; KCND2; up-frameshift protein1; arrhythmia

Received 12 November 2024, accepted 22 May 2025

[1]*Department of Pharmacology (The Key Laboratory of Cardiovascular Research, Ministry of Education) at College of Pharmacy, Harbin Medical University, Harbin 150086, China*
[2]*Department of Cardiology, the First Affiliated Hospital, Harbin Medical University, Harbin 150001, China*
[3]*Institute for Frontier Medical Technology, Shanghai University of Engineering Science, Shanghai 201620, China*
[4]*Research Unit of Noninfectious Chronic Diseases in Frigid Zone, Chinese Academy of Medical Sciences, Beijing 100730 ,China*
[5]*Key Laboratory of Cell Transplantation, The First Affiliated Hospital, Harbin Medical University, Harbin 150001, China*

[*]*Corresponding authors Zhenwei Pan, E-mail: panzw@ems.hrbmu.edu.cn; Dongmei Gong, E-mail: gdmxxl@163.com; Yue Li, E-mail: ly99ly@hrbmu.edu.cn*
[#]*These authors contributed equally to this work*

1 Introduction

J-Wave syndrome (JWS) is characterized by distinctive J-waves on the electrocardiogram[1] and is strongly associated with an increased risk of life-threatening ventricular arrhythmias[2]. The J-wave arises from the notch of the ventricular action potential, which is mainly determined by the transmural gradient of the transient outward potassium current (I_{to}) and the sodium current (I_{Na}). J-waves are commonly observed in brugada (BrS) and early repolarization syndromes (ERS)[3]. I_{to} is predominantly expressed in the subepicardial myocytes, generating voltage gradient between epicardial and endocardial myocytes during the early phase of the action potential. This gradient is particularly pronounced in the right ventricle and underlies the formation of J-waves[4]. Consistently, loss-of-function mutations in the sodium channel gene *SCN5A* in patients with idiopathic ventricular fibrillation re associated with prominent J-waves on the electrocardiogram (ECG)[5]. Exposure to cold environments

has been shown to affect the kinetics of key cardiac ion channels and is a well-established trigger for cardiac electrical instability, particularly in individuals with underlying channelopathies. Systemic hypothermia or localized cold stress can induce or accentuate J-waves, and is associated with an elevated risk of malignant ventricular arrhythmias[6-7]. Despite advances in our understanding of JWS, its precise molecular mechanisms remain to be elusive.

Long noncoding RNAs (lncRNAs) are single-strand RNAs longer than 200 nucleotides that lack protein-coding capacity. They play essential regulatory roles in cardiovascular diseases, including myocardial infarction[8], heart failure[9] and cardiac arrhythmia[10-12]. LncRNAs modulate diverse electrophysiological properties of cardiomyocytes including excitation conduction[11], membrane repolarization[13] and automaticity[14]. Dysregulation of lncRNAs can contribute to arrhythmogenesis by altering the expression and function of ion channels[15]. However, the involvement of lncRNA in JWS remains unknown.

In our previous work, we identified a cardioprotective lncRNA, named Cardiac Injury-Related Bclaf1-Inhibiting lncRNA (lncCIRBIL)[16]. Interestingly, during electrocardiographic recordings, we unexpectedly observed prominent J-waves in lncCIRBIL knockout mice. This prompted us to investigate the role of lncCIRBIL in JWS. In the present study, we demonstrate that lncCIRBIL regulates J-wave formation by modulating up-frameshift protein1 (UPF1) mediated *KCND2* mRNA degradation and thereby controlling the transmural heterogeneity of I_{to} in the right ventricle. These findings reveal that lncCIRBIL as a novel electrophysiology-specific functional subclass of lncRNAs. Distinct from structural remodeling pathways, lncCIRBIL uniquely regulates ion channel heterogeneity through UPF1-dependent mRNA decay.

2 Methods

Detailed descriptions of materials and experimental procedures are provided in the Supplementary Material.

3 Results

3.1 LncCIRBIL deficiency is associated with J-point elevation and increased arrhythmia susceptibility

We firstly assessed the ECG waveforms in lncCIRBIL knockout (lncCIRBIL-KO) mice. J-waves were observed more frequently in lncCIRBIL-KO mice 20/22 compared with wild-type (WT) controls 13/23 (Fig. 1A, 1B). Quantitative analysis of the downward deflection slope of the J-wave demonstrated a significantly more negative derivative in lncCIRBIL-KO mice than in WT mice (Fig. 1C). Since accentuated J-waves were closely associated with increased arrhythmia vulnerability[17], we next assessed ventricular arrhythmia susceptibility using programmed electrical stimulation. Ventricular tachycardia (VT) and ventricular fibrillation (VF) were inducible in 11 of 14 lncCIRBIL-KO mice, compared with only 2 of 14 WT mice (Fig. 1D, 1E). Furthermore, VT/VF duration was significantly longer in lncCIRBIL-KO mice relative to WT controls (Fig. 1F).

Previous studies have shown that transmural gradients of potassium and sodium currents contribute to J-wave syndrome[18]. We therefore examined expression patterns of *KCND2, KCND3, KCNIP2* and *SCN5A* in the right and left ventricles of WT and lncCIRBIL-KO mice. Notably, the transmural difference of *KCND2* was dramatically increased in the right ventricle of lncCIRBIL-KO mice, while *KCND3*, *KCNIP2* and *SCN5A* showed no significant changes (Fig. 1G-1J). In contrast, no significant differences in the transmural expression of *KCND2, KCND3, KCNIP2,* or *SCN5A* were detected in the left ventricle (Fig. 1K-1N). To exclude structural heart disease as a confounding factor, we examined cardiac morphology by hematoxylin-eosin (HE) staining, which showed no detectable abnormalities (Supplementary Fig. 3A-3C). Echocardiographic assessment further revealed that lncCIRBIL deletion had no significant effect on ejection fraction (EF) or fractional shortening (FS) (Supplementary Fig. 3D-3F). Collectively, these results indicate that lncCIRBIL deficiency promotes J-wave formation and increases arrhythmia susceptibility, likely by enhancing the transmural heterogeneity of *KCND2* in the right ventricle.

3.2 Transmural differences in transient outward current (I_{to}) are amplified in lncCIRBIL-KO mice

To further assess the impact of lncCIRBIL knockout on Ito, we performed voltage-clamp recordings in right ventricular myocytes. In WT mice, Ito was larger in subepicardial than in subendocardial myocytes, and this transmural difference was significantly amplified in lncCIRBIL-KO mice (Fig. 2A-C). Consistently, Kv4.2 protein expression was higher in subepicardial compared with subendocardial cardiomyocytes of the right ventricle, and this difference was further augmented by lncCIRBIL deletion (Fig. 2D-F). In line with these findings, action potential recordings showed a further shortening of APD in subepicardial versus subendocardial myocytes of the right ventricle in lncCIRBIL-KO mice compared with WT controls (Fig. 2G-M). However, no significant differences were observed in action potential amplitude (APA), resting membrane potential (RP), or overshoot (OS) between WT and lncCIRBIL-KO right ventricular myocytes (Fig. 2N-P). By contrast, no significant differences in I_{to} or action potential parameters were detected between subendocardial and subepicardial cardiomyocytes of the left ventricle in either WT or lncCIRBIL-KO mice (Supplementary Fig. 4A-C). Collectively,

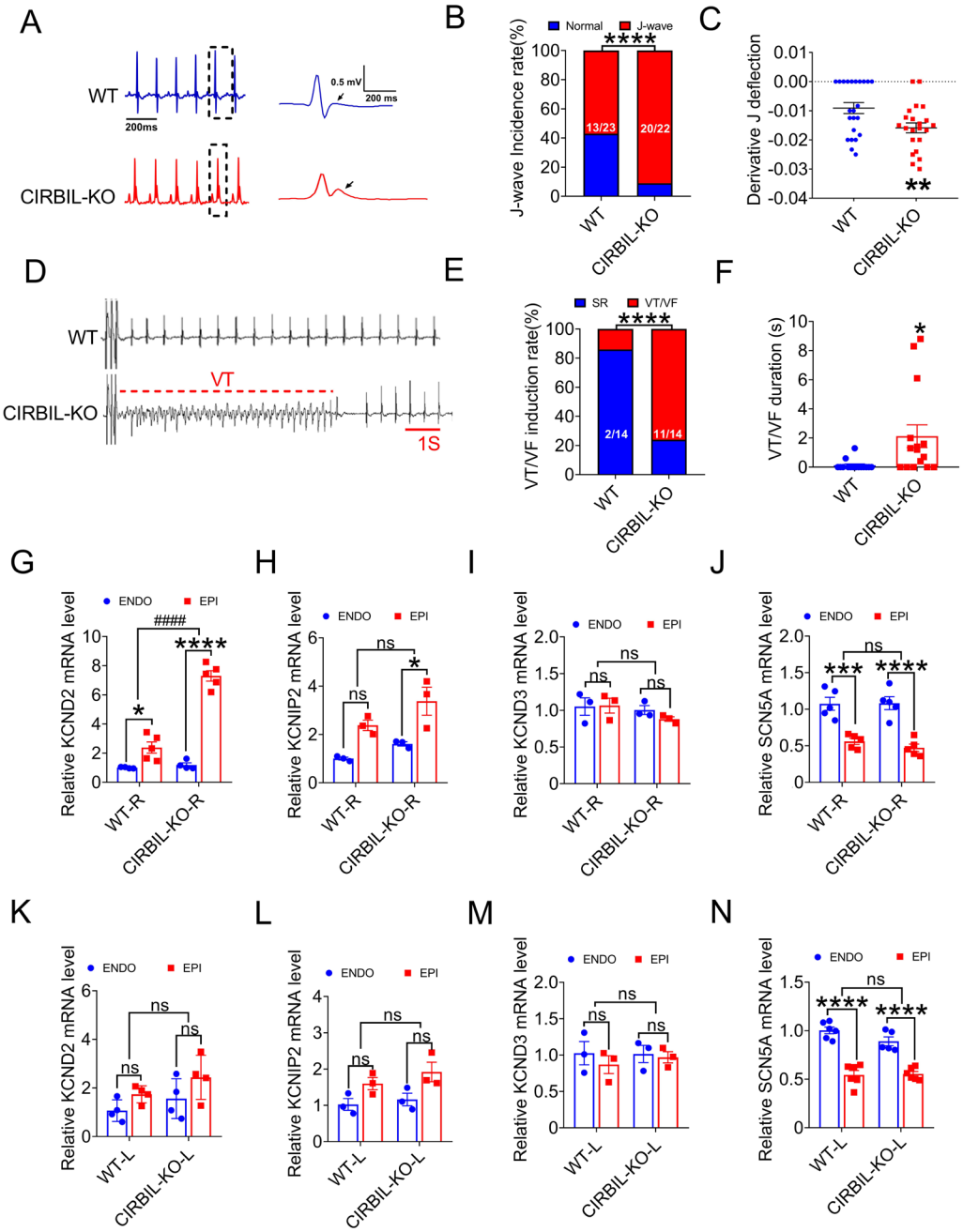

Fig. 1 Surface ECGs showing arrhythmias in WT and Cardiac lncCIRBIL knockout mice

(A) Representative lead II surface ECGs from WT and CIRBIL-KO mice. Right panels show magnified boxed regions highlighting typical J-waves (arrows). (B) Incidence of J-waves in lead II of WT (N = 23) and CIRBIL-KO (N = 22) mice. $^{****}P < 0.0001$ versus WT mice. Fisher's exact test. (C) Average values of the derivative of J-wave downward deflection in lead II of WT (N = 23) and CIRBIL-KO (N = 22) mice. $^{**}P < 0.01$ versus WT, unpaired t test. (D) Representative example of VT induced by programmed. stimulation. (E, F) Induction rate and duration of VT/VF following programmed stimulation in WT and CIRBIL-KO mice (N = 14 per group). $^{*}P < 0.05$, $^{****}P < 0.0001$ versus WT, Fisher's exact test and unpaired t test. (G-N) mRNA expression levels of *KCND2*, *KCNIP2*, *KCND3*, and *SCN5A* in EPI and ENDO cardiomyocytes of WT-R, CIRBIL-KO-R and WT-L, CIRBIL-KO-L from WT and CIRBIL-KO mice (N = 3-6 per group). $^{*}P < 0.05$, $^{***}P < 0.001$, $^{****}P < 0.0001$, $^{\#\#\#\#}P < 0.0001$, two-way ANOVA followed by Bonferroni's multiple comparisons test. Data are expressed as mean ± SEM. Data are expressed as mean ± SEM. Electrocardiograms, ECGs; WT, Wild Type; CIRBIL-KO, CIRBIL Knockout; HR, Heart Rate; WT-R, Right Ventricle of WT; CIRBIL-KO-R, Right Ventricle of CIRBIL-KO; WT-L, Left Ventricle of WT; CIRBIL-KO-L, Left Ventricle of CIRBIL-KO; ENDO, Endocardial Cardiomyocytes; EPI, Epicardial Cardiomyocytes.

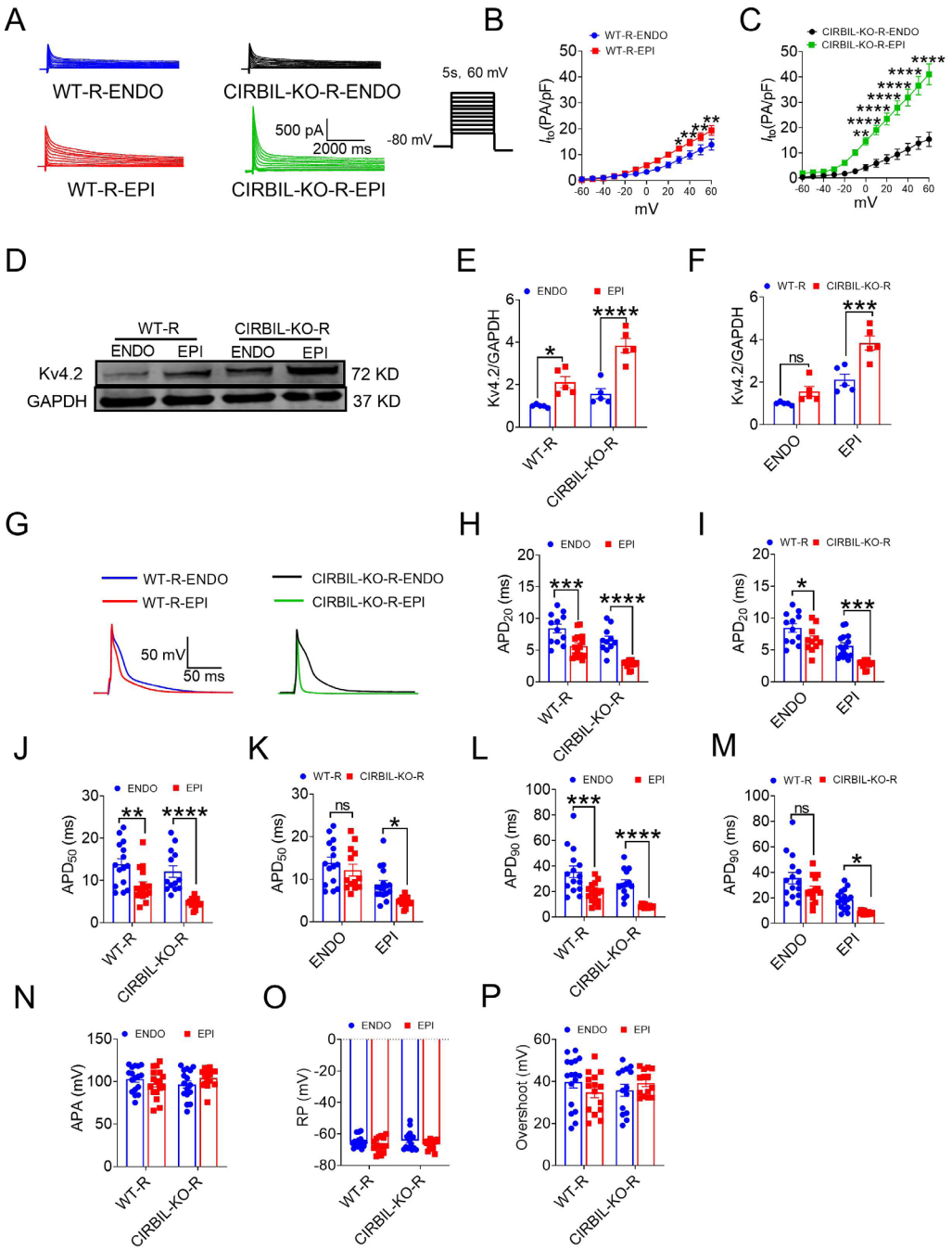

Fig. 2 Effects of lncCIRBIL knockout on transmural differences of I_{to} and APD in the right ventricle

(A-C) Representative current traces and I-V relationships of I_{to} in EPI and ENDO myocytes of right ventricle from WT (N = 8) and CIRBIL-KO (N = 9) mice. $^{*}P < 0.05$, $^{**}P < 0.01$, $^{****}P < 0.0001$ versus ENDO; two-way ANOVA followed by Bonferroni's post hoc test. (D-F) Kv4.2 protein levels in EPI and ENDO myocytes from WT-R and CIRBIL-KO-R mice (N = 5 per group). $^{*}P < 0.05$, $^{***}P < 0.001$, $^{****}P < 0.0001$ versus ENDO; two-way ANOVA followed by Bonferroni's post hoc test. (G) Representative AP recordings from EPI and ENDO myocytes of WT-R and CIRBIL-KO-R mice. (H-P) Quantitative analyses of AP parameters, including APD_{20}, APD_{50}, APD_{90}, APA, RP, and OS. Quantitative data are presented as mean ± SEM. $^{*}P < 0.05$, $^{**}P < 0.01$, $^{***}P < 0.001$ and $^{****}P < 0.0001$ versus ENDO; two-way ANOVA with Bonferroni's post hoc test. WT, Wild Type; CIRBIL-KO, CIRBIL Knockout; WT-R, Right Ventricle of WT; CIRBIL-KO-R, Right Ventricle of CIRBIL-KO; EPI, Epicardial Cardiomyocytes; ENDO, Endocardial Cardiomyocytes; APD, Action Potential Duration; APA, Action Potential Amplitude; RP, Resting Membrane Potential; OS, Overshoot.

these results demonstrate that lncCIRBIL deficiency selectively enhanced the transmural heterogeneity of I_{to} in the right ventricle.

3.3 Transgenic overexpression of lncCIRBIL reduces J-wave amplitude and the transmural I_{to} heterogeneity in the right ventricle

To further investigate the role of lncCIRBIL, we generated cardiac-specific lncCIRBIL transgenic (lncCIRBIL-TG) mice (Supplementary Fig. 1). LncCIRBIL overexpression significantly decreased the frequency of J-waves compared with WT controls (Fig. 3A-C). Voltage-clamp recordings showed that the transmural gradient of I_{to} between subepicardial and subendocardial myocytes in the right ventricle was markedly reduced in lncCIRBIL-TG mice relative to WT mice (Fig. 3D-F). Consistently, lncCIRBIL overexpression significantly reduced the levels of *KCND2* mRNA and Kv4.2 protein in right ventricular subepicardium and abolished their transmural differences (Fig. 3G-H). In line with the effects of lncCIRBIL on I_{to}, the differences in APD between subepicardial and subendocardial myocytes of the right ventricle were diminished in lncCIRBIL-TG mice (Fig. 3I-L). By contrast, APA, RP, and OS of right ventricular myocytes were not significantly altered (Fig. 3M-O). Together, these results demonstrate that transgenic overexpression of lncCIRBIL suppresses J-wave formation by reducing transmural Ito heterogeneity in the right ventricle.

3.4 LncCIRBIL binds to UPF1 to regulate *KCND2* mRNA stability

We next explored the molecular mechanism by which lncCIRBIL regulates *KCND2* expression. Since lncCIRBIL is localized in the cytosol[16] and its altered expression affected *KCND2* mRNA levels, we hypothesized that lncCIRBIL m modulates *KCND2* mRNA stability through interactions with cytoplasmic proteins. Interestingly, in our previous RNA pulldown-mass spectrometry analysis, the mRNA decay-related factor UPF1 was identified as a lncCIRBIL-associated protein[16], suggesting it could mediate *KCND2* mRNA degradation. To validate this interaction, we performed RNA pulldown and RNA immunoprecipitation (RIP) assays. The sense, but not antisense, sequence of lncCIRBIL successfully pulled down UPF1 (Fig. 4A), and UPF1 antibody precipitated lncCIRBIL in RIP assays (Fig. 4B).

We next evaluated whether UPF1 was responsible for *KCND2* mRNA degradation and how lncCIRBIL influenced this process. Silencing UPF1 significantly increased the half-life of *KCND2* mRNA (Fig. 4C). Similarly, lncCIRBIL knockdown in neonatal mouse ventricular myocytes prolonged *KCND2* mRNA half-life (Fig. 4D), whereas lncCIRBIL overexpression shortened it (Fig. 4E).

RIP assays further showed that UPF1 antibody precipitated *KCND2* mRNA in WT mice, but not in lncCIRBIL-KO mice (Fig. 4F-G). To explore direct interactions between lncCIRBIL and *KCND2* mRNA, we performed RNA-RNA pulldown using biotin-labeled probes followed by RT-qPCR. The schematic plasmid constructs used for the assay are shown in Fig. 4H. LncCIRBIL, but not the negative control S1m, successfully pulled down *KCND2* mRNA (Fig. 4I). Notably, lncCIRBIL was still able to bind *KCND2* mRNA in the absence of UPF1 (Fig. 4J). These results suggest that lncCIRBIL directly binds *KCND2* mRNA, while UPF1 recruitment to *KCND2* mRNA requires lncCIRBIL.

The 7-methyl-guanosine (m^7G) cap at the 5' end of eukaryotic mRNAs protects transcripts from exonuclease-mediated degradation, and decapping is the critical initial step in mRNA decay. Since UPF1-mediated decay typically requires mRNA decapping[19], we examined *KCND2* mRNA decapping. Decapping of *KCND2* mRNA was significantly reduced in lncCIRBIL-KO mice, whereas it was markedly enhanced in lncCIRBIL-TG mice (Fig. 4K). Importantly, UPF1 protein levels were unchanged in both epicardial and endocardial tissues of WT and lncCIRBIL-KO right ventricles (Fig. 4L). Together, these findings indicate that lncCIRBIL binds UPF1 and directly interacts with *KCND2* mRNA, thereby recruiting UPF1 to promote *KCND2* mRNA decapping and degradation.

3.5 Effects of the human homologous conserved fragment of lncCIRBIL (hcf-CIRBIL) on *KCND2*

LncCIRBIL is an intergenic lncRNA consisting of 862 nucleotides (nts) located on chromosome 6 (Supplementary Fig. 5). Sequence alignment with the human genome identified a conserved 407-nt motif, designated as the human conserved fragment of lncCIRBIL (hcf-CIRBIL) (Supplementary Fig. 5A-B). Notably, plasma levels of hcf-CIRBIL were significantly lower in patients with J-wave syndrome compared with control subjects (Fig. 5A). Consistent with the findings in mice, hcf-CIRBIL successfully pulled down UPF1 in both human AC16 cardiomyocyte cells and mouse heart tissue (Fig. 5B). Functionally, overexpression of hcf-CIRBIL in AC16 cells significantly decreased *KCND2* mRNA and protein levels (Fig. 5C), whereas knockdown of hcf-CIRBIL led to a marked upregulation of *KCND2* expression (Fig. 5D). Together, these data suggest that the conserved human fragment of lncCIRBIL (hcf-CIRBIL) exerts regulatory effects on *KCND2* expression through a mechanism involving UPF1, paralleling the role of mouse lncCIRBIL.

We next examined the functional role of hcf-CIRBIL in human induced pluripotent stem cell-derived cardiomyocytes (hiPSC-CMs). Knockdown of hcf-CIRBIL significantly increased I_{to} (Fig. 6A-B), enhanced the action potential notch, and shortened APD_{20} (Fig. 6C-F). Conversely, overexpression of hcf-CIRBIL

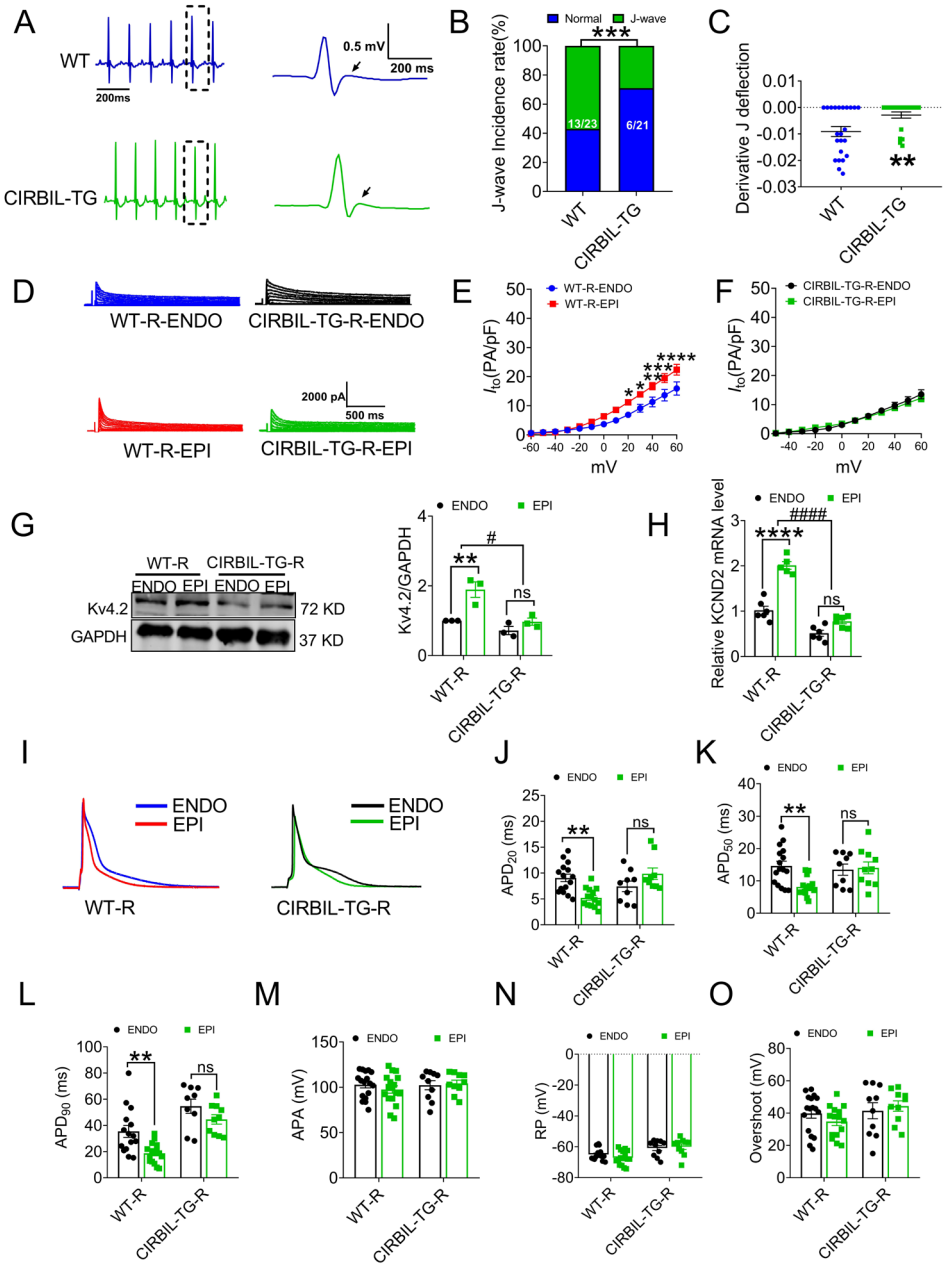

Fig. 3 Cardiomyocyte-specific transgenic overexpression of lncCIRBIL attenuates J-wave syndrome

(A) Representative lead II surface ECGs from WT and CIRBIL-TG mice. Right panels show magnified boxed regions highlighting reduced J-wave amplitude (arrows) in CIRBIL-TG mice. (B) Incidence of J-waves in lead II of WT (N = 23) and CIRBIL-TG (N = 21) mice. $^{***}P < 0.001$ versus WT, Fisher's exact test. (C) Average values of the derivative of J-wave downward deflection in lead II of WT (N = 23) and CIRBIL-TG (N = 21) mice. $^{**}P < 0.01$ versus WT mice; unpaired t test. (D) Representative I_{to} traces from EPI and ENDO cardiomyocytes of the right ventricle. (E, F) I-V relationships of I_{to} in right ventricular cardiomyocytes from WT (N = 15) and CIRBIL-TG (N = 17) mice. $^{*}P < 0.05$, $^{**}P < 0.01$, $^{***}P < 0.001$, $^{****}P < 0.0001$ versus ENDO; two-way ANOVA followed by Bonferroni's post hoc test. (G) Kv4.2 protein expression in EPI and ENDO myocytes of WT-R and CIRBIL-TG-R mice (N = 3 per group). $^{**}P < 0.01$, $^{\#}P < 0.05$. (H) *KCND2* mRNA levels in EPI and ENDO myocytes of WT-R and CIRBIL-TG-R mice (N = 5-6 per group). $^{****}P < 0.0001$, $^{\#\#\#\#}P < 0.0001$. (I) Typical APD traces from EPI and ENDO cardiomyocytes of WT-R and CIRBIL-TG-R mice. (J-O) Quantitative analyses of APD_{20}, APD_{50}, APD_{90}, APA, RP, and OS in WT and CIRBIL-TG right ventricular cardiomyocytes (N = 17 per group). $^{**}P < 0.01$, $^{***}P < 0.001$; two-way ANOVA with Bonferroni's post hoc test. Data are presented as mean ± SEM. WT, Wild Type; CIRBIL-TG, lncCIRBIL Transgenic Mice; WT-R, Right Ventricle of WT; CIRBIL-TG-R, Right Ventricle of CIRBIL-TG; ENDO, Endocardial Cardiomyocytes; EPI, Epicardial Cardiomyocytes; APD, Action Potential Duration; APA, Action Potential Amplitude; RP, Resting Potential; OS, Overshoot.

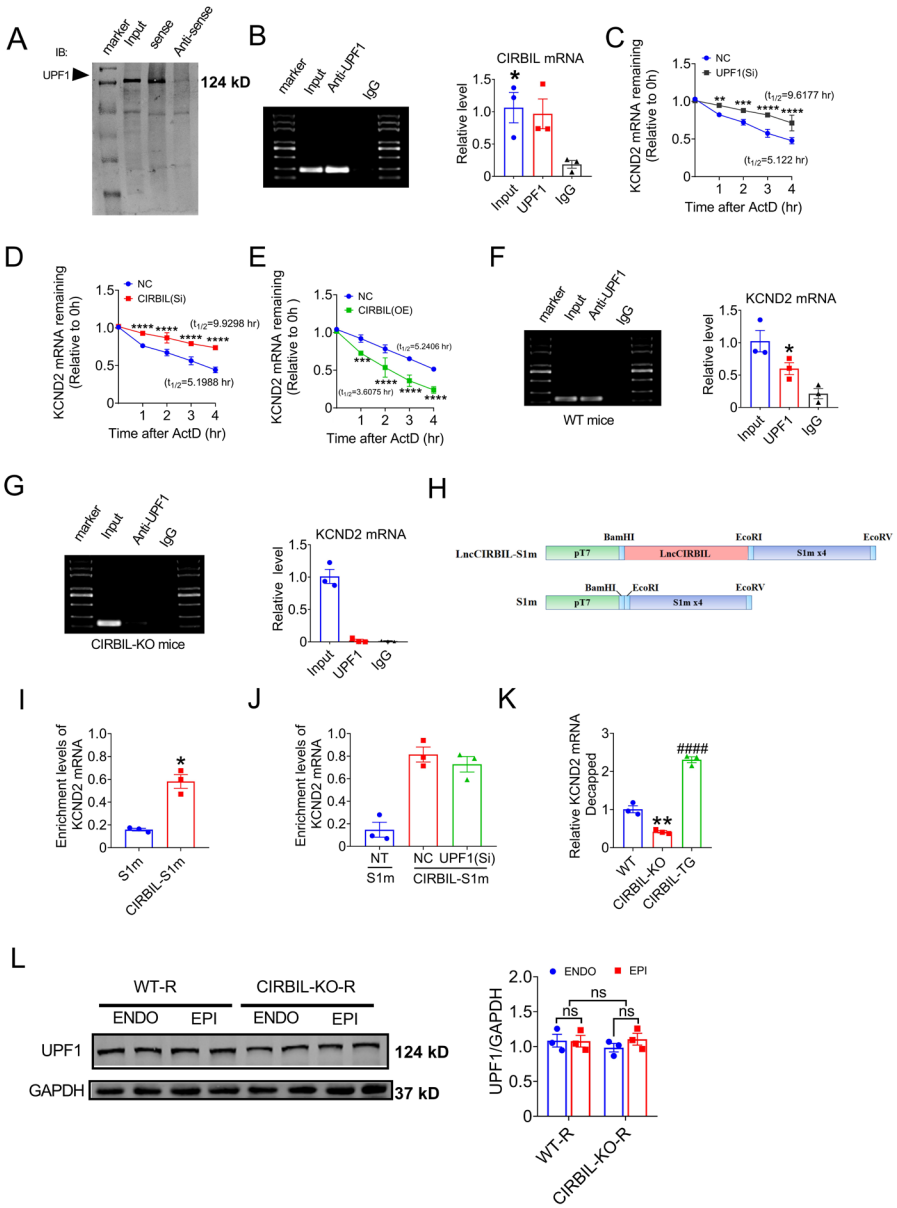

Fig. 4 LncCIRBIL binds to UPF1 and regulates KCND2 mRNA stability

(A) Western blot analysis of UPF1 pulled down by lncCIRBIL. (B) RNA immunoprecipitation (RIP) showing enrichment of lncCIRBIL using UPF1 antibody in mouse heart tissue (*N* = 3 per group). $^{*}P < 0.05$ versus IgG group, unpaired *t* test. (C) *KCND2* mRNA decay in neonatal mouse ventricular myocytes after UPF1 knockdown. Cells were treated with 5 μg/mL actinomycin D (ActD) for the indicated times; RNA levels were quantified by RT-qPCR. *N* = 3 independent experiments. $^{**}P < 0.01$, $^{***}P < 0.001$, $^{****}P < 0.001$ versus NC, student's *t* test. (D, E) Effects of lncCIRBIL silencing or overexpression on *KCND2* mRNA decay. *N* = 3 independent experiments. $^{***}P < 0.001$, $^{****}P < 0.0001$ versus NC, student's *t* test. (F, G) RIP showing enrichment of *KCND2* mRNA with UPF1 antibody in cardiac tissue from WT and CIRBIL-KO mice (*N* = 3 per group). $^{*}P < 0.05$ versus IgG group, one-way ANOVA followed by Bonferroni's post hoc test. (H) Schematic illustration of S1m-plasmid constructs with or without lncCIRBIL. (I) RNA pulldown showing interaction between lncCIRBIL and *KCND2* mRNA. *N* = 3 independent experiments. $^{*}P < 0.05$ versus S1m control, student's *t* test. (J) RNA pulldown assay showing lncCIRBIL-*KCND2* interaction after UPF1 knockdown (*N* = 3 independent experiments). (K) Decapping of *KCND2* mRNA in hearts of WT, CIRBIL-KO, and CIRBIL-TG mice, measured by qRT-PCR (*N* = 3 per group). $^{**}P < 0.01$ for CIRBIL-KO versus WT; $^{\#\#\#\#}P < 0.0001$ for CIRBIL-TG versus WT; one-way ANOVA followed by Bonferroni post hoc test. (L) UPF1 protein levels in EPI and ENDO myocytes of WT-R and CIRBIL-KO-R mice (*N* = 3 per group). Data are presented as mean ± SEM. WT, Wild Type; CIRBIL-KO, CIRBIL Knockout Mice; CIRBIL-TG, CIRBIL Transgenic Overexpression Mice; WT-R, Right Ventricle of Wild Type Mice; CIRBIL-TG-R, Right Ventricle of CIRBIL Transgenic Overexpression Mice; AD, ActD, Actinomycin; EPI, Epicardial Cardiomyocytes; ENDO, Endocardial Cardiomyocytes; NC, Negative Control.

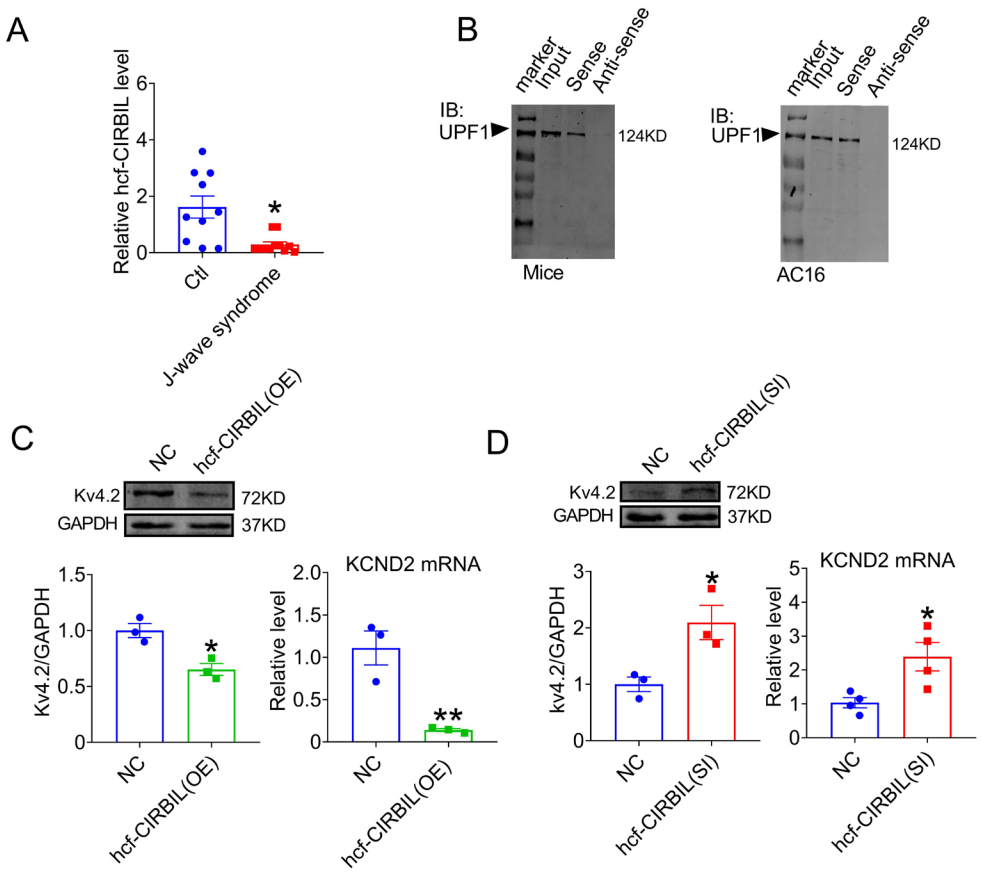

Fig. 5 Binding of hcf-CIRBIL to UPF1 and its influence on KCND2 in AC16 cells

Plasma levels of hcf-CIRBIL in patients with J-wave syndrome (*N* = 10) and healthy controls (*N* = 11), measured by qRT-PCR. $^{*}P < 0.05$ versus Ctl, unpaired *t* test. (B) Pulldown assays showing binding of UPF1 by hcf-CIRBIL in mouse heart tissue and human AC16 cells. (C) Effects of hcf-CIRBIL overexpression on Kv4.2 protein and *KCND2* mRNA expression in AC16 cells. qRT-PCR: *N* = 4; western blot: *N* = 3; each from 3 independent experiments. $^{*}P < 0.05$, $^{**}P < 0.01$ versus negative control (NC), Student's *t* test. (D) Effects of hcf-CIRBIL knockdown on Kv4.2 protein and *KCND2* mRNA expression in AC16 cells. *N* = 3 independent experiments. $^{*}P < 0.05$ versus NC, Student's *t* test. Data are expressed as mean ± SEM. hcf-CIRBIL, Human Conserved Fragment of lncCIRBIL; NC, Negative Control; Ctl, Control Subjects.

reduced I_{to} (Fig. 6G-H), attenuated action potential notch, and prolonged APD_{20} (Fig. 6I-6L). Moreover, transfection of hcf-CIRBIL significantly reduced the decay half-life of *KCND2* mRNA (Fig. 6M). These data imply that hcf-CIRBIL is a critical regulator of I_{to} in human cardiomyocytes and may contribute to the pathogenesis of J-wave syndrome.

3.6 Transgenic lncCIRBIL overexpression alleviates cold-induced JWS and ventricular arrhythmia susceptibility in mice

To further explore the functional role of lncCIRBIL in JWS, we established a cold-induced JWS model by exposing mice to cold temperature (4 °C ± 1 °C) for 4 weeks. Plasma lncCIRBIL levels were significantly reduced in cold-exposed mice compared with those maintained at room temperature (25 °C ± 1 °C) (Fig. 7A). Cold exposure markedly increased the incidence of J-point elevation in WT mice (20 of 23 at 4 ± 1 °C versus 10 of 23 at 25 ± 1 °C). In contrast, cardiomyocyte-specific transgenic overexpression of lncCIRBIL significantly suppressed J-point elevation, which was observed in only 7 of 21 CIRBIL-TG mice exposed to 4 ± 1 °C (Fig. 7B-D). Consistently, cold exposure substantially increased the incidence of ventricular arrhythmias in WT mice, whereas lncCIRBIL overexpression dramatically reduced arrhythmia susceptibility (Fig. 7E-G). At the molecular level, cold exposure enhanced *KCND2* mRNA and Kv4.2 protein expression in subepicardial compared with subendocardial myocardium of the right ventricle (Fig. 7H-J). Taken together, these results demonstrate that lncCIRBIL overexpression mitigates cold-induced J-wave augmentation and arrhythmia vulnerability by preventing the enhancement of transmural heterogeneity in the right ventricle.

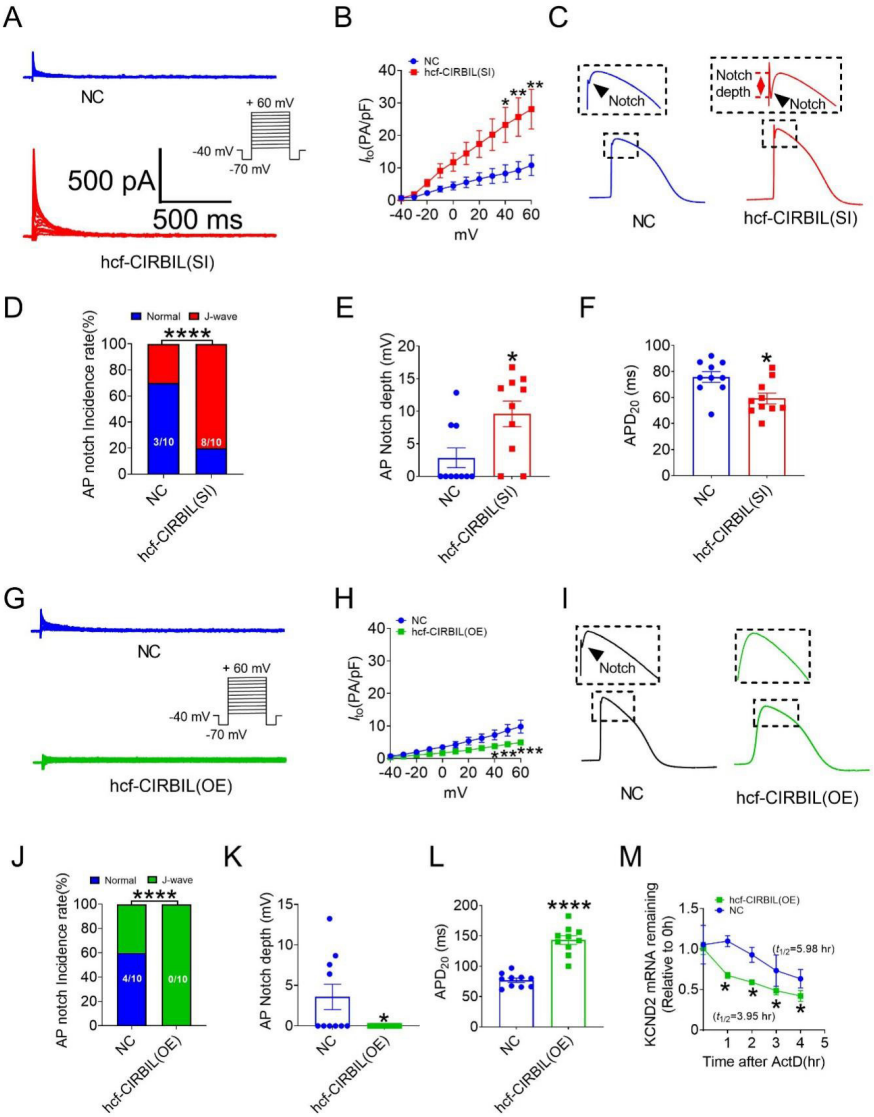

Fig. 6 Effects of hcf-CIRBIL on KCND2 expression and function in hiPSC-derived cardiomyocytes (hiPSC-CMs)

(A, B) Effects of hcf-CIRBIL knockdown on I_{to} in hiPSC-CM (N = 10 cells per group). $^{*}P < 0.05$, $^{**}P < 0.01$ versus NC; two-way ANOVA comparison followed by Bonferroni's post hoc test. (C-E) Effects of hcf-CIRBIL(SI) knockdown (siRNA, SI) on notching incidence rate and AP notch depth in hiPSC-CM (N = 10 cells per group). $^{*}P < 0.05$ versus NC., by student's t-test. Notching incidence was compared using Fisher's exact test. $^{****}P < 0.0001$ versus NC. (F) Effects of hcf-CIRBIL knockdown on APD_{20} (N = 10 cells per group). $^{*}P < 0.05$ versus NC, student's t-test. (G, H) Effects of hcf-CIRBIL overexpression on I_{to} in hiPSC-CM. $^{*}P < 0.05$, $^{**}P < 0.01$, $^{***}P < 0.001$ versus NC; two-way ANOVA with Bonferroni's post hoc test. (I-L) Effects of hcf-CIRBIL overexpression on notching incidence rate and AP notch depth in hiPSC-CM (N = 10 cells per group). $^{*}P < 0.05$ versus NC, student's t-test. Notching incidence compared by Fisher's exact test. $^{****}P < 0.0001$ versus NC. (M) Effects of hcf-CIRBIL overexpression on decay half-life of *KCND2* mRNA in hiPSC-CM treated with 5 ug/ml ActD (N = 3 independent experiments). $^{*}P < 0.05$ for hcf-CIRBIL(OE) vs NC, student's t-test. Data are expressed as mean ± SEM. hcf-CIRBIL, Human Conserved Fragment of lncCIRBIL; hiPSC-CM, Human Induced Pluripotent Stem Cell-Derived Cardiomyocyte; NC, Negative Control; SI, Small Interfering RNA Knockdown; OE, Overexpression; APD20, Action Potential Duration at 20% Repolarization; ActD, Actinomycin D.

4 Discussion

In this study, we demonstrated that lncCIRBIL deficiency amplifies transmural heterogeneity of I_{to} in the right ventricle, thereby increasing J-wave incidence and arrhythmia susceptibility. Conversely, cardiomyocyte-specific transgenic overexpression of lncCIRBIL attenuated cold-induced J-waves and reduced right ventricular I_{to} gradients. Mechanistically, lncCIRBIL facilitated *KCND2* mRNA degradation through direct interaction with UPF1, leading to suppression of I_{to} (Fig. 8). Together, these findings

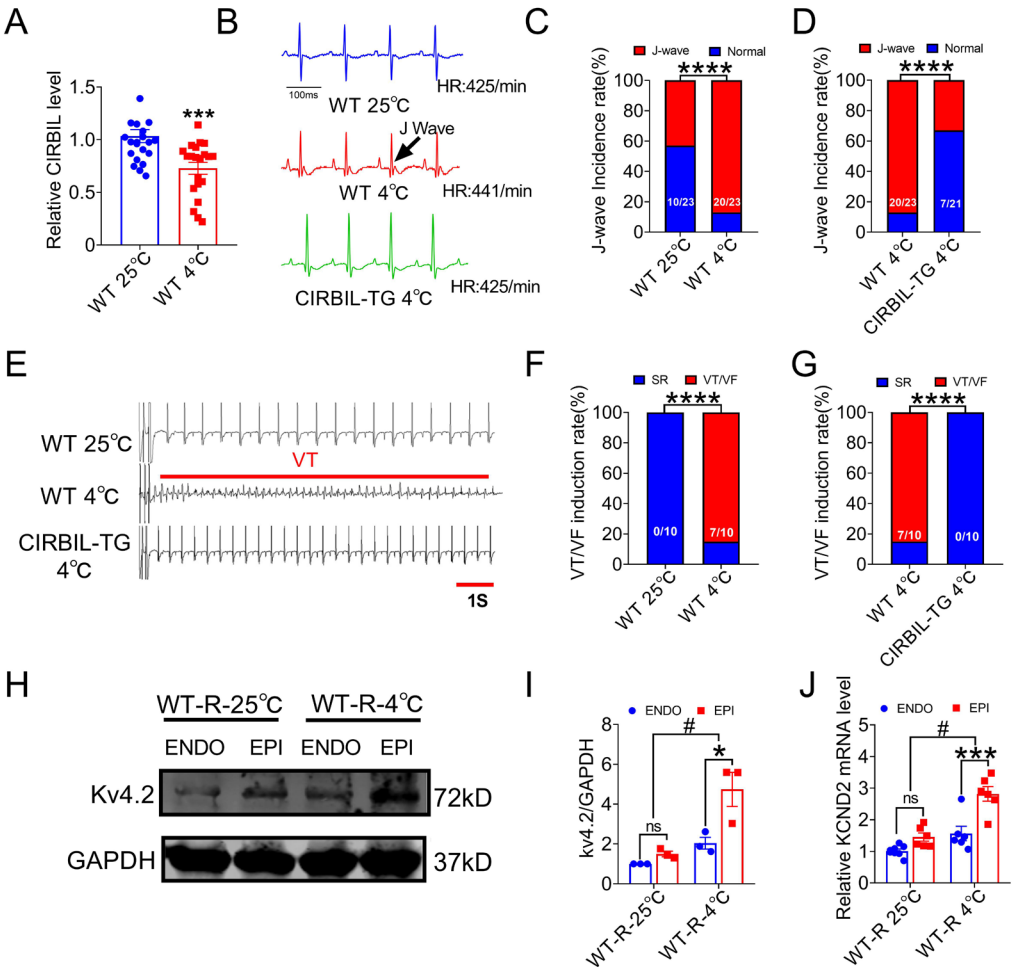

Fig. 7 LncCIRBIL overexpression suppresses cold-induced J-point elevation and ventricular arrhythmia susceptibility

(A) Plasma lncCIRBIL levels in mice maintained at 4 ± 1 °C (*N* = 21) versus 25 ± 1 °C (*N* = 22), measured by qRT-PCR. $^{***}P < 0.001$ versus WT 25°C±1 °C, unpaired *t* test. (B-D) Representative lead II ECGs from WT and CIRBIL-TG mice exposed to 25 ± 1 °C or 4 ± 1 °C, and incidence of J-wave elevation. *N* = 23 for WT mice maintained at 4°C ± 1 °C, *N* = 23 for WT mice maintained at 25 °C ± 1 °C. $^{****}P < 0.0001$ versus WT 25°C±1 °C, $^{****}P < 0.0001$ versus WT 4 °C ± 1 °C, Fisher's exact test. (E-G) Representative ECGs and incidence of VT/VF induced by programmed stimulation (*N* = 10 mice per group). VF/VT inducibility was compared by Fisher's exact test. $^{****}P < 0.0001$ versus WT 25 °C ± 1 °C, $^{****}P < 0.0001$ versus WT at 4 °C. (H-J) Kv4.2 protein and *KCND2* mRNA expression in epicardial (EPI) and endocardial (ENDO) myocytes of right ventricles from WT mice exposed to 25 °C or 4 °C. qRT-PCR: *N* = 6; western blot: *N* = 3. $^{*}P < 0.05$, $^{***}P < 0.001$ versus WT-R-ENDO, $^{\#}P < 0.05$ versus WT-R 25°C; two-way ANOVA with Bonferroni's post hoc test. Data are expressed as mean ± SEM. WT, Wild Type; CIRBIL-TG, lncCIRBIL Transgenic Mice; WT-R, Right Ventricle of WT; CIRBIL-TG-R, Right Ventricle of CIRBIL-TG; EPI, Epicardial Cardiomyocytes; ENDO, Endocardial Cardiomyocytes; VT, Ventricular Tachycardia; VF, Ventricular Fibrillation.

identify lncCIRBIL as a critical regulator of J-wave syndrome and highlight its contribution to ventricular arrhythmia vulnerability.

4.1 Involvement of lncCIRBIL in JWS

The role of lncRNAs in cardiac arrhythmogenesis has gained increasing attention in recent years. For example, Zhang *et al.* reported that lncCCRR prevents ventricular arrhythmia by upregulating connexin43 and improving gap junction conduction[11]. Similarly, lnc-KCNA2as upregulation decreases KCNA2 mRNA and Kv1.2 protein in rats with chronic heart failure[20], lncRNA TCONS-00106987 promotes atrial electrical remodeling during atrial fibrillation via miR-26-mediated regulation of KCNJ2[10]. In the present study, we found that lncCIRBIL deficiency significantly increased J-wave incidence and arrhythmia inducibility in mice, whereas circulating lncCIRBIL levels were markedly reduced in patients with JWS. These observations establish lncCIRBIL as a novel player in cardiac electrophysiology. Importantly, plasma lncCIRBIL quantification may serve as a potential biomarker for JWS risk stratification, although further large-scale validation is required. Mechanisms underlying lncCIRBIL regulation of JWS.

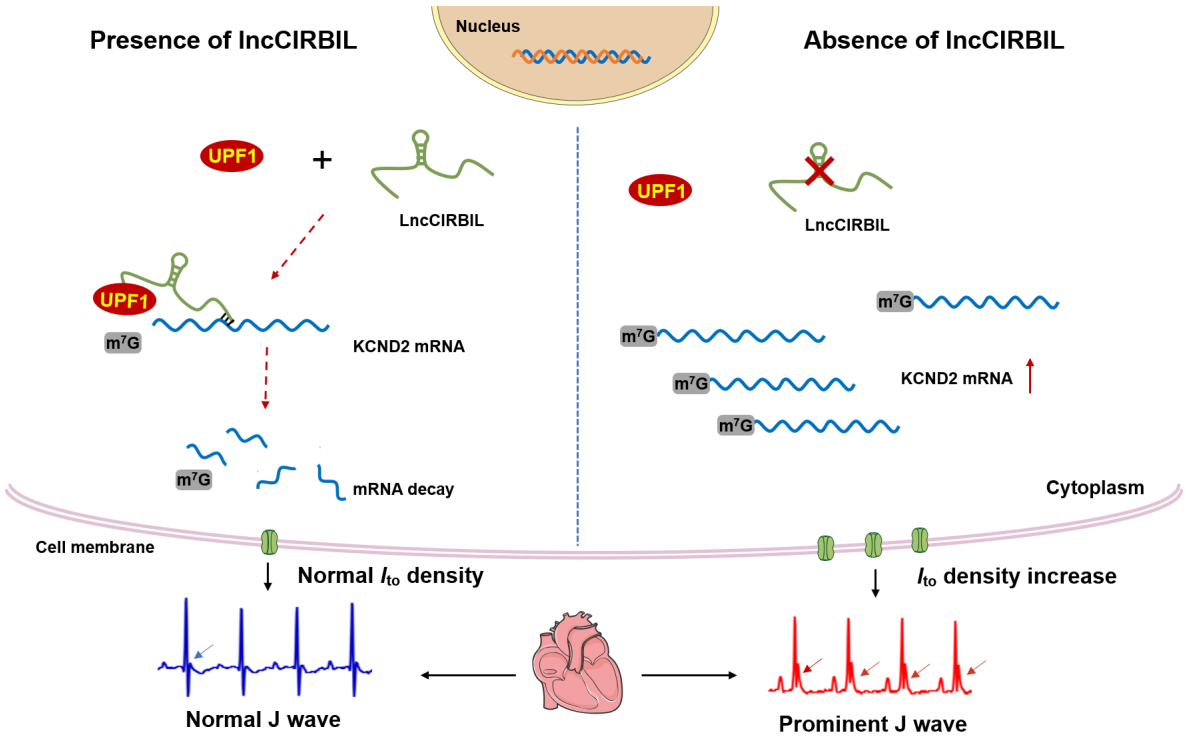

Fig. 8 Proposed mechanism by which lncCIRBIL regulates J-wave syndrome

LncCIRBIL binds and recruits UPF1 to promote *KCND2* mRNA decay in cardiomyocytes. Reduction of lncCIRBIL impairs UPF1-mediated degradation of *KCND2* mRNA, leading to increased Ito density and enhanced transmural heterogeneity in the right ventricle, which predisposes to J-wave syndrome. UPF1, up-frameshift protein1; lncCIRBIL, Injury-Related Bclaf1-Interacting LncRNA. The figure was drawn by the BioRender (Toronto, Canada).

JWS has been linked to disturbances in multiple ionic currents, including INa, Ito, and ICaL. Yan *et al*. provided the first direct evidence that heterogeneous Ito distribution across the ventricular wall generates the spike-and-dome action potential morphology, which underlies J-wave manifestation on the ECG[4]. Epicardial Ito-mediated action potential notching, absent in endocardium, produces a transmural voltage gradient that registers as J-waves or J-point elevation[21]. Moreover, Christiaan *et al*. showed that Hey2 haploinsufficiency diminishes Ito and I_{Na} gradients, leading to attenuated J-waves[22]. Similarly, IRX5, a transcriptional regulator of potassium channel genes, is essential for maintaining Ito gradients and coordinated repolarization[23].

Our results are consistent with these mechanistic insights: lncCIRBIL deficiency enhanced Ito and shortened action potential duration in right ventricular epicardium compared with endocardium, in parallel with increased *KCND2* mRNA and Kv4.2 protein expression. These findings align with human cardiac transcriptome data showing higher *KCND2* expression in right ventricular epicardium relative to endocardium, but no comparable gradient in the left ventricle[24]. Furthermore, in hiPS-CM, silencing of lncCIRBIL shortened APD and accentuated AP notching, reinforcing the role of lncCIRBIL in regulating I_{to} heterogeneity and J-wave formation.

4.2 Regulatory mechanisms of lncCIRBIL on *KCND2*

A key mode of action for lncRNAs involves interaction with specific proteins to modulate their function[25]. UPF1 is a central effector of RNA surveillance and degradation, best known for its role in nonsense-mediated decay (NMD)[26]. Beyond NMD, UPF1 also regulates normal mRNAs through pathways involving RNA-binding proteins such as staufen, glucocorticoid receptor, regnase-1, and Tudor-staphylococcal/micrococcal-like nucleases [27]. More recently, UPF1 has been implicated in the rapid degradation of m6A-modified RNAs[28]. LncRNAs are likewise critical regulators of mRNA decay and stability [29]. For example, lncRNA 1/2-sbsRNAs induces decay of complementary mRNAs via STAU1 recruitment[30] while lncICR[31] and SNHG5[32] enhance mRNA stabilization via partial base-pairing with ICAM-1 and SPATS2 mRNA, respectively. Importantly, UPF1 has been shown to act in concert with lncRNAs; Lee *et al*. demonstrated that linc-ASEN cooperates with UPF1 to modulate *p21* mRNA stability[33].

Our study identifies a unique mechanism whereby lncCIRBIL

facilitates UPF1-mediated *KCND2* mRNA degradation through m7G cap-dependent decay. Specifically, lncCIRBIL recruits UPF1 to promote removal of the protective 5′ m7G cap, thereby exposing *KCND2* mRNA to exonucleolytic degradation. In contrast, lncCIRBIL deficiency disrupts UPF1 recruitment, allowing *KCND2* transcripts to retain their protective cap and accumulate, ultimately enhancing Ito density and transmural heterogeneity.

4.3 Effects of lncCIRBIL on cold-exposure induced JWS

J-waves are known to be augmented by hypothermia. Yamaki *et al.* showed that low ambient temperature triggers J-wave syndromes and increases arrhythmia vulnerability, which can be prevented by I_{to} inhibition or environmental warming[34]. In line with these findings, we observed that cold exposure significantly increased J-wave incidence and ventricular arrhythmia susceptibility in WT mice. Notably, these effects were substantially alleviated by cardiomyocyte-specific overexpression of lncCIRBIL, highlighting its protective role against cold-induced electrophysiological disturbances.

5 Study limitations

This study has several limitations. First, human cardiac tissues were not available, and plasma samples from patients with J-wave syndrome were limited in number. Larger clinical cohorts are required to validate the diagnostic and prognostic utility of lncCIRBIL in JWS. Second, although our data strongly support UPF1-mediated decay as the primary mechanism of *KCND2* regulation, other factors may contribute. Future transcriptome-wide approaches such as RNA interactome capture and CLIP-seq will be necessary to identify additional lncCIRBIL-interacting proteins or alternative mechanisms, including transcriptional regulation or splicing modulation.

6 Conclusion

Our study identifies lncCIRBIL as a critical regulator of J-wave syndrome. Deficiency of lncCIRBIL amplifies transmural I_{to} heterogeneity by impairing UPF1-mediated *KCND2* mRNA degradation, leading to J-wave formation and heightened arrhythmia susceptibility. Conversely, lncCIRBIL overexpression attenuates J-wave augmentation under both basal and cold-induced conditions. These findings reveal a novel molecular mechanism underlying J-wave syndrome and underscore the clinical relevance of lncCIRBIL as both a biomarker and a potential therapeutic target.

Acknowledgements

Not applicable.

Research ethics

The use of human samples was approved by the Institutional Review Board of College of Pharmacy, Harbin Medical University (IRB2007821) and complies with the requirements of the Declaration of Helsinki. All protocols for animal experiments were approved by the Committee for Animal Experimentation of Harbin Medical University (IRB2007821) and complies with the requirements of the Declaration of Helsinki.

Informed consent

Written informed consent of each participant was obtained.

Author contributions

Pan Z W, Gong D M and Li Y conceived the study concept. Jin X X, Ma W B, Guo J Y, Qu Y Y, Gao H Y, Yin D C, Li D S, Shi L, Li J L, Ma J D, Zhang L M, Shan H L, Lu Y J performed the experimental studies. Jin X X, Ma W B and Guo J Y carried out the data analysis. Pan Z W, Jin X X and Ma W B wrote the manuscript. Pan Z W, Jin X X and Yin D C provided the funding. All authors reviewed the manuscript. Jin X X, Ma W B and Guo J Y contributed equally to this work.

Use of large language models, AI and machine learning tools

Not applicable.

Conflict of interests

Pan Z W is an Editorial Board Member of Frigid Zone Medicine. The article was subject to the journal's standard procedures, with peer review handled independently of this Member and his research groups.

Research funding

This work was supported by National Natural Science Foundation of China (82270320 to Yin D C; 82300280 to Jin X X; 82070344, 81870295 to Pan Z W), HMU Marshal Initiative Funding (HMUMIF-21017 to Pan Z W), Excellent Young Medical Talents Training Fund of the First Affiliated Hospital of Harbin Medical University (No. 2024YQ03 to Jin X X).

Data availability

The data are presented in the study and further inquiries can be directed to the corresponding author.

References

[1] Macfarlane P W, Antzelevitch C, Haissaguerre M, *et al*. The early repolarization pattern: a consensus paper. J Am Coll Cardiol, 2015; 66(4): 470-477.

[2] Antzelevitch C, Yan G X. J wave syndromes. Heart Rhythm, 2010; 7(4): 549-558.

[3] Antzelevitch C, Yan G X. J-wave syndromes: brugada and early repolarization syndromes. Heart Rhythm, 2015; 12(8): 1852-1866.

[4] Yan G X, Antzelevitch C. Cellular basis for the electrocardiographic J wave. Circulation, 1996; 93(2): 372-379.

[5] Remme C A, Verkerk A O, Hoogaars W M, *et al*. The cardiac sodium channel displays differential distribution in the conduction system and transmural heterogeneity in the murine ventricular myocardium. Basic Res Cardiol, 2009; 104(5): 511-522.

[6] Kim S H, Kim D Y, Kim H J, *et al*. Early repolarization with horizontal ST segment may be associated with aborted sudden cardiac arrest: a retrospective case control study. BMC Cardiovasc Disord, 2012; 12: 122.

[7] Lee W S, Nam G B, Kim S H, *et al*. ECG features and proarrhythmic potentials of therapeutic hypothermia. Heart, 2016; 102(19): 1558-1565.

[8] Ponnusamy M, Liu F, Zhang Y H, *et al*. Long noncoding RNA CPR (Cardiomyocyte Proliferation Regulator) regulates cardiomyocyte proliferation and cardiac repair. Circulation, 2019; 139(23): 2668-2684.

[9] Gao R, Wang L, Bei Y, *et al*. Long noncoding RNA cardiac physiological hypertrophy-associated regulator induces cardiac physiological hypertrophy and promotes functional recovery after myocardial ischemia-reperfusion injury. Circulation, 2021; 144(4): 303-317.

[10] Du J, Li Z, Wang X, *et al*. Long noncoding RNA TCONS-00106987 promotes atrial electrical remodelling during atrial fibrillation by sponging miR-26 to regulate KCNJ2. J Cell Mol Med, 2020; 24(21): 12777-12788.

[11] Zhang Y, Sun L, Xuan L, *et al*. Long non-coding RNA CCRR controls cardiac conduction via regulating intercellular coupling. Nat Commun, 2018; 9(1): 4176.

[12] Babapoor-Farrokhran S, Gill D, Rasekhi R T. The role of long noncoding RNAs in atrial fibrillation. Heart Rhythm, 2020; 17(6): 1043-1049.

[13] Bertaso F, Sharpe C C, Hendry B M, *et al*. Expression of voltage-gated K + channels in human atrium. Basic Res Cardiol, 2002; 97(6): 424-433.

[14] Yang B, Lin H, Xiao J, *et al*. The muscle-specific microRNA miR-1 regulates cardiac arrhythmogenic potential by targeting GJA1 and KCNJ2. Nat Med, 2007; 13(4): 486-491.

[15] Yeh C F, Chang Y E, Lu C Y, *et al*. Expedition to the missing link: long noncoding RNAs in cardiovascular diseases. J Biomed Sci, 2020; 27(1): 48.

[16] Zhang Y, Zhang X, Cai B, *et al*. The long noncoding RNA lncCIRBIL disrupts the nuclear translocation of Bclaf1 alleviating cardiac ischemia-reperfusion injury. Nat Commun, 2021; 12(1): 522.

[17] Behr E R. J-wave syndromes, SCN5A, and cardiac conduction reserve: two sides of the same coin? J Am Coll Cardiol, 2021; 78(16): 1618-1620.

[18] Antzelevitch C, Di Diego J M. J wave syndromes: what's new? Trends Cardiovasc Med, 2021; 32(6): 350-363.

[19] He F, Jacobson A. Control of mRNA decapping by positive and negative regulatory elements in the Dcp2 C-terminal domain. RNA, 2015; 21(9): 1633-1647.

[20] Long Q Q, Wang H, Gao W, *et al*. Long noncoding RNA Kcna2 antisense RNA contributes to ventricular arrhythmias via silencing kcna2 in rats with congestive heart failure. J Am Heart Assoc, 2017; 6(12): E005965.

[21] Badri M, Patel A, Yan G X. Cellular and ionic basis of J-wave syndromes. Trends Cardiovasc Med, 2015; 25(1): 12-21.

[22] Veerman C C, Podliesna S, Tadros R, *et al*. The brugada syndrome susceptibility gene HEY2 modulates cardiac transmural ion channel patterning and electrical heterogeneity. Circ Res, 2017; 121(5): 537-548.

[23] Kim K H, Oh Y, Liu J, *et al*. Irx5 and transient outward K(+) currents contribute to transmural contractile heterogeneities in the mouse ventricle. Am J Physiol Heart Circ Physiol, 2022; 322(5): H725-H741.

[24] Gaborit N, Le Bouter S, Szuts V, *et al*. Regional and tissue specific transcript signatures of ion channel genes in the non-diseased human heart. J Physiol, 2007; 582(Pt 2): 675-693.

[25] Bridges M C, Daulagala A C, Kourtidis A. LNCcation: lncRNA localization and function. J Cell Biol, 2021; 220(2): E202009045.

[26] Hwang H J, Park Y, Kim Y K. UPF1: from mRNA surveillance to protein quality control. Biomedicines, 2021; 9(8): 995.

[27] Kim Y K, Maquat L E. UPFront and center in RNA decay: UPF1 in nonsense-mediated mRNA decay and beyond. RNA, 2019; 25(4): 407-422.

[28] Gibbs M R, Chanfreau G F. UPF1 adds an m(6)A feather to its (de) cap. Cell Rep, 2022; 39(8): 110898.

[29] Yoon J H, Abdelmohsen K, Gorospe M. Posttranscriptional gene regulation by long noncoding RNA. J Mol Biol, 2013; 425(19): 3723-3730.

[30] Gong C, Maquat L E. lncRNAs transactivate STAU1-mediated mRNA decay by duplexing with 3' UTRs via Alu elements. Nature, 2011; 470(7333): 284-288.

[31] Guo W, Liu S, Cheng Y, *et al*. ICAM-1-Related noncoding RNA in cancer stem cells maintains ICAM-1 expression in hepatocellular carcinoma. Clin Cancer Res, 2016; 22(8): 2041-2050.

[32] Damas N D, Marcatti M, Come C, *et al*. SNHG5 promotes colorectal cancer cell survival by counteracting STAU1-mediated mRNA destabilization. Nat Commun, 2016; 7: 13875.

[33] Lee H C, Kang D, Han N, *et al*. A novel long noncoding RNA Linc-ASEN represses cellular senescence through multileveled reduction of p21 expression. Cell Death Differ, 2020; 27(6): 1844-1861.

[34] Yamaki M, Sato N, Imanishi R, *et al*. Low room temperature can trigger ventricular fibrillation in J wave syndromes. HeartRhythm Case Rep, 2016; 2(4): 347-350.